



Predicting Shear Capacity of Panel Zone Using Neural Network and Genetic Algorithm

M. Vajdian^a, S. M. Zahrai^{*b}, S. M. Mirhosseini^a, E. Zeighami^a

^a Department of Civil Engineering, Arak Branch, Islamic Azad University, Arak, Iran

^b Center of Excellence for Engineering and Management of Civil Infrastructures, School of Civil Engineering, College of Engineering, University of Tehran, Tehran, Iran

PAPER INFO

Received 07 March 2020
Received in revised form 03 May 2020
Accepted 12 June 2020

Keywords:

Box-Shaped Cross-Sections
Genetic Algorithm
Neural Network
Shear Capacity of Panel Zone
Steel moment-Resisting Frame

ABSTRACT

Investigating the behavior of the box-shaped column panel zone has been one of the major concerns of scientists in the field. In the American Institute of Steel Construction the shear capacity of I-shaped cross-sections with low column thickness is calculated. This paper determines the shear capacity of panel zone in steel columns with box-shaped cross-sections by using artificial neural network (ANN) and genetic algorithm (GA). It also compares ABAQUS finite element software outputs and AISC relations. Therefore, neural networks were trained using parametric information obtained from 510 connection models in ABAQUS software. The results show that the predicted shear capacity of the NN and the GA in comparison with the AISC relations use a wide range of all effective parameters in the calculation of the shear capacity of panel zone. Therefore, the use of artificial intelligence can be a good choice. Finally, the GA, along with optimization of a mathematical relation, has been able to minimize the error in determining the shear capacity of panel zones of steel-based columns, even at high column thicknesses.

doi: 10.5829/ije.2020.33.08b.09

1. INTRODUCTION

In recent decades, connections have been one of the most important concerns of scientists in the field. The major differences of recent approaches are paying more attention to the beam-to-column load transfer path and ensuring that this load transfer path is safe to the extent of the lateral load system behavior. Therefore, this study focuses on research and predicts the shear capacity of panel zones in steel boxes using NN method. Seismic behavior of panel zones has been the focus of numerous researchers for a long time. Research has begun in the late 1960s and early 1970s. In the last four decades, significant changes have been observed in the seismic design criteria of panel zones. Over the years, there have been many changes to panel zone by laws and guidelines. The 2002 AISC seismic criterion stated that the shear resistance required by panel zone must be determined by testing. In other words, it does not provide a quantitative

relationship. However, as a minimum, the shear resistance required of panel zone must be determined from the sum of bending moments in the column resulting from the formation of expected bending moments at the points of formation of plastic hinge [1]. The 2010 AISC Seismic Code is the latest and the most up-to-date version of the seismic design criteria for steel structures. In the section on panel zones sections of the special bending reinforced frames, no changes were considered compared to the 2002 AISC criteria [2]. Mansouri et al. [3] proved that the AISC relations overestimate in I-shaped columns with relatively thick flanges. What seems to be necessary is that the shear capacity of panel zone depends primarily on the various geometrical parameters of the coupling components and, secondly, the AISC relations have acceptable errors for I-shaped cross-sections with low thicknesses. However, these errors became more pronounced at higher thicknesses and box-shaped cross-sections [3]. Today,

*Corresponding Author Institutional Email: mzahrai@ut.ac.ir
(S. M. Zahrai)

NNs are used in almost all engineering sciences. NNs, also known as ANNs, are one of the learning algorithms in "machine learning" that are based on the biological concept of NNs. ANNs are the building blocks or neurons, very simple computing devices. Communication between neurons determines network function. The purpose of ANN training is to determine the appropriate relationship for solving different problems [4]. Many researchers have used ANN to study structures, for instance Hartman et al. [5] have investigated the use of ANN in assessing different levels of structures safety. Elhewy et al. [6] have investigated the ability of NNs to predict the failure of structures.

Optimization techniques include the recently developed random search methods. Among the new optimization techniques used today to solve many different problems are GA (GA), Simulated Annealing (SA), Ant Colony and more. Regardless of the type of calculation, these methods can be applied at different levels of engineering. In these methods, simple algorithms are used for complex calculations [7]. Jenkins' research [8] is one of the first studies in optimizing structures. Adeli [9] also explored the use of NNs to improve the responses of GAs to optimization problems. Sahoo and Maity [10] used a combination of NN and GA to predict structural damage .

Khalkhali et al [11] proved that neural networks are useful tools to predict the buckling capacity of vertically stiffened cylindrical shells.

Mallela et al [12] dealt with the development of an analytical and computationally efficient analysis tool using artificial neural networks (ANN) for predicting the buckling load of laminated composite stiffened panels subjected to in-plane shear loading. The results show that the trained neural network can predict the shear buckling load of laminated composite stiffened panels accurately and will be very useful in optimization applications [12].

Abmbres et al. [13] proposed an artificial neural network (ANN)-based formula to come up with estimates of the shear capacity of one-way reinforced concrete slabs under a concentrated load. A step-by-step assessment scheme for reinforced concrete slab bridges by means of the ANN-based model is also proposed, which results in an improvement of the current assessment procedures [13].

Hoang [14] relied on a piecewise multiple linear regression (PMLR) and artificial neural network (ANN) approaches to construct a prediction model that can approximate the mapping function between the punching shear capacity of SFRC flat slabs and its influencing factors. The algorithms of gradient descent and Levenberg-Marquardt backpropagation were employed to train the ANN based prediction models. Experimental results showed that SPMLR can deliver prediction outcome which was better than those of ANN as well as empirical design equations [14].

Jang et al. [15] reported the magnitudes of fiber optic sensor signals were used for estimating the distances between each sensor and impact location. Then, through the neural network training, the accuracy of estimating the distances from the signal magnitudes could be enhanced. Triangulation method showed the acceptable localization results about the non-trained impact points [15].

Hedayat et al. [16] were aimed to propose an integrated formula developed based on artificial neural network to predict the minimum resistance requirement of steel moment frames at any performance level and desired level of probabilistic response. In addition to the simple form of the proposed model, results generally indicated that this model was more accurate than the other available models [16].

In recent decades, due to the widespread use of these cross-sections in moment-resisting frame systems, investigating the behavior of the box-shaped column panel zone has been one of the major concerns of scientists in the field. As a rectangular area of column web, panel zone is enclosed between continuity plates and column flanges and plays an important role in the bonding behavior. The shear capacity of this region depends on various parameters, such as the geometrical dimensions of the beam cross-section, the geometrical dimensions of the column cross-section and the thickness of continuity plates. In the American Institute of Steel Construction (AISC), based on these parameters, the shear capacity of I-shaped cross-sections with low column thickness is calculated. However, no separate relations have been provided to determine the shear capacity of panel zone in metal columns with box-shaped cross-sections. The error of the AISC relations is particularly evident at high thicknesses. This paper determines the shear capacity of panel zone in metal columns with box-shaped cross-sections with artificial neural network (ANN) and genetic algorithm (GA). It also compares ABAQUS finite element software outputs and AISC relations. The parameters used to determine this shear capacity are height, flange thickness, beam and column thickness, thickness of continuity plates and axial force of the column.

In this study, an ANN and GA are designed to calculate the shear capacity of panel zone-loaded steel columns for the purpose of a separate relationship and reducing the errors mentioned in the AISC. To achieve this goal, first, an extensive parametric study is performed on the parameters affecting the performance of the connection source by ABAQUS software. These parameters include column flange thickness, column web thickness, beam flange thickness, column width, height of beam and thickness of continuity plates. Then, an ANN is designed and trained based on ABAQUS software outputs. This network is examined to predict the shear capacity of square columns or boxes with low to

high thickness ranges. The results are compared with the ABAQUS output and the AISC. Then, using the GA, an optimal function is determined to predict and calculate the shear capacity of the bending steel columns. After that, the performance of artificial intelligence in relation to the AISC relations is investigated in terms of shear capacity of the box-shaped columns with different column thicknesses.

2. CALCULATING THE SHEAR CAPACITY OF PANEL ZONE

2. 1. Calculating the Shear Capacity of Panel Zones in American Institute of Steel Construction (AISC)

The AISC Relations, based on the Crawler Relations, yielded an acceptable result for relatively thin columns. However, for high column flange thicknesses, these relations need to be modified. It is important to note that the difference in shear capacity of panel zone is due to the high thickness and shape of the cross-section, so that the column with the box-shaped cross-section is not specified in the AISC as separate relation [17]. In recent AISC seismic design standards based on the LRFD design, the design resistance of panel zones is classified as follows, with or without the deformation of panel zones depending on the axial force applied to the column [2]:

A) When the deformation effect of panel zones is not considered in the frame, R_n is the capacity of panel zones as follows:

$$R_n = 0.6F_y \cdot d_c \cdot t_w \quad P_r \leq 0.4P_c \quad (1)$$

$$R_n = 0.6F_y \cdot d_c \cdot t_w \left(1.4 - \frac{P_r}{P_c}\right) \quad P_r > 0.4P_c \quad (2)$$

B) When considering the deformation effect of panel zone in the frame, the capacity of panel zone is as follows:

In Equations (1) to (4), the first part deals with the yield point and the second part concerns the final capacity of panel zone. In the above equations, F_y is the yield stress of column cross-section, d_c is column cross depth, t_w is column web thickness, b_{cf} is column flange width, t_{cf} is column flange thickness, d_b is column depth, P_r is column design resistance and P_c is column axial yield resistance.

It can be stated that the AISC uses five physical parameters of panel zone to calculate the shear capacity. These parameters are: 1) Depth of column, 2) Thickness of column, 3) Width of column, 4) Thickness of column, 5) Depth of beam.

Figure 1 shows the calculated values of V_{pz} , shear capacity based on the AISC relations for 510 specimens. V_{pz} is the shear capacity of panel zone named R_n in the AISC.

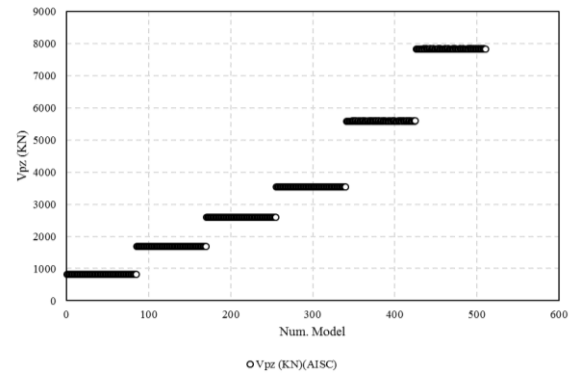


Figure 1. Shear capacity based on the AISC relations for 510 samples

2. 2. Finite Elements Modeling

2. 2. 1. Modeling Verification

In this part, in order to ensure the accuracy of the numerical results of the performed analysis, a steel beam to column connection performed by Stojadinović et al. [18] is modeled in ABAQUS. In the following, the mentioned model is analyzed and the results of this analysis are compared to laboratory results [18].

2. 2. 2. Geometrical Properties and Materials of the Laboratory Specimens

The laboratory specimen was built from a column with the $W14 \times 120$ section; and for the beam, a $W24 \times 68$ section was used. The model geometry and loading details are shown in Figure 2. The used materials in this experiment are steel plates for the stiffeners, beams, and columns with the yield resistance of 358 MPa and ultimate tensile resistance of 475 MPa as shown in Table 1.

$$R_n = 0.6 F_y \cdot d_c \cdot t_w \left(1 + \frac{3b_{cf} \cdot t_{cf}^2}{d_b \cdot d_c \cdot t_w}\right) \quad P_r \leq 0.75P_c \quad (3)$$

$$R_n = 0.6 F_y \cdot d_c \cdot t_w \left(1 + \frac{3b_{cf} \cdot t_{cf}}{d_b \cdot d_c \cdot t_w}\right) \left(1.9 - \frac{1.2P_r}{P_c}\right) \quad P_r > 0.75P_c \quad (4)$$

2. 2. 3. Meshing

In order to model the beam, column and the stiffener plates, the shell and solid elements were used. Also, the modeled geometry was partitioned for regular meshing with the partitioning command.

2. 2. 4. Boundary Condition and Loading

The boundary condition of the laboratory specimen requires that the displacement of all the nodes in the above and below the column were tightly restrained. Also, for the out-of-plane buckling, the beam was restrained. All the boundary and support conditions are applied in modeling. The loading was in the form of displacement application to the beam end with the amount of 195 mm.

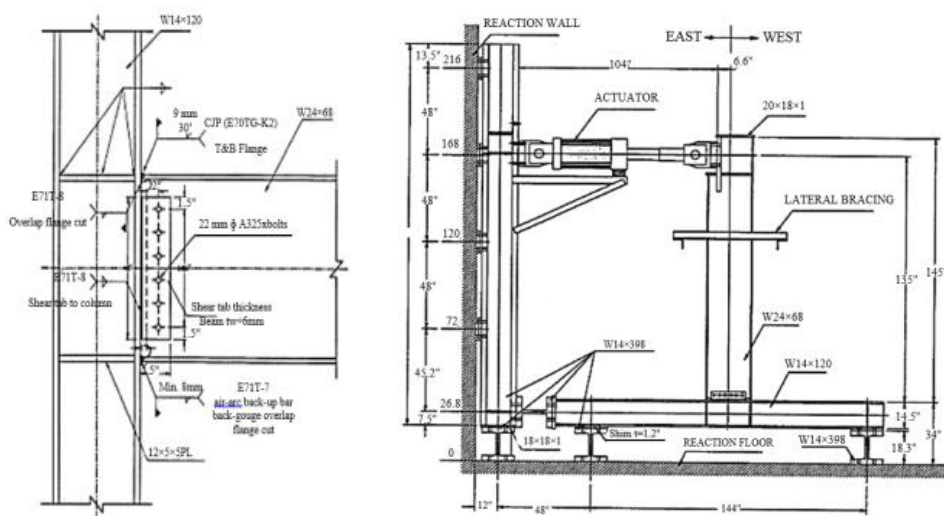


Figure 2. Specimen geometry specifications

TABLE 1. The specifications of the materials used in the experiment

Young's modulus (GPa)	Poisson's Ratio	Ultimate Tensile Resistance (MPa)	Yield Resistance (MPa)	Material
210	0.3	475	358	Steel

2. 2. 5. The Results of the Load-Displacement Analysis

The answers of load-final displacement resulted from the analysis results for the numerical sample with the answers of the load-displacement of the laboratory specimen are illustrated in Figure 3. As it can be observed in this figure, the load-displacement curves are almost coincident. In fact, from the beginning, the aim of the sample calibration was to accommodate the load-displacement curve of the numerical model with the laboratory sample.

2. 2. 6. Parametric Studies with ABAQUS Software and Calculation of Shear Capacity of Panel Zones

ABAQUS software version 2017 was used for parametric modeling and calculation of shear capacity of panel zone. In this part of the research, the details of modeling using finite element method are presented. In this section, the model made in the previous section is used for modeling, with the exception of the box-shaped column instead of the H-shaped column. In the models, it is assumed that the steel beam-column connections are rigid and welded. Variable parameters are used in modeling 510 models, namely change in beam flange thickness, beam web, continuity plate, column web thickness and column flange thickness. The boundary conditions are similar to the model boundary conditions made in the previous section. Four thicknesses of 8, 10, 15 and 20 mm were

used for the beam flange, beam web and continuity plate thickness parameters. In addition, 6 thicknesses of 8, 10, 15, 20, 30 and 40 mm were used for column web and column flange thickness (Table 2).

The beam and column dimensions used in parametric studies are I500X250 and BOX400X400, respectively. For the used material in this study, the yield resistance of 345 MPa and ultimate tensile resistance of 510 MPa are assumed.

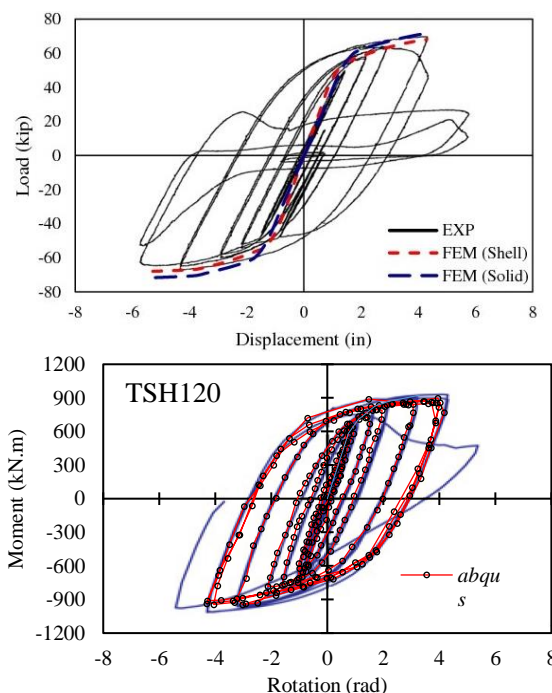


Figure 3. Comparison of load-displacement results for the numerical model and the experimental specimen

TABLE 2. Dimensions of parametric study models

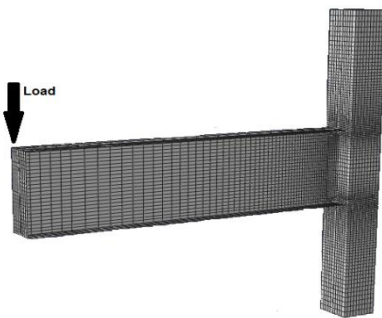
Model	$t(mm)$
Beam flange	
Beam web	8,10,15,20
Continuity Plate	
Column flange	8,10,15,20,30,40
Column web	

The boundary conditions of the parametric models were such that the displacement of all the nodes located at the top and bottom of the column which was constrained to be clamped. In addition, it was bound for the buckling off the beam plate. The loading was applied to the end of the beam by a displacement of 150 mm. The steel beam connections are rigid and welded. Therefore, the 9 cross-sectional geometrical parameters for calculating the shear capacity of panel zones are effective: 1) column length, 2) column width, 3) column flange thickness, 4) column web thickness, 5) beam flange width, 6) beam height (x to X beam flange), 7) beam flange thickness, 8) beam web thickness, and 9) thickness of panel zone stiffeners. To accelerate the modeling process, the S4R quadruple shell element was used to construct the cross-sections. To improve the accuracy, in the areas close to the connection and panel zones, a fine mesh was selected. In all cases, 3500 mm beam length and 3000 mm column length were considered. Figure 4 shows an overview of the model built into ABAQUS software.

In the modeling performed, the proposed equations in literature [19] are used to calculate panel zone cut. In addition, the equations proposed in literature [20] are used to calculate the shear strain of panel zone.

$$V_{pz} = \frac{PL}{h_t} \left(1 - \frac{h_t}{H}\right) \quad (5)$$

$$\gamma = \frac{\Delta^+ + \Delta^-}{2} \left(\frac{\sqrt{d_{pz}^2 + b_{pz}^2}}{d_{pz} b_{pz}} \right) \quad (6)$$

**Figure 4.** An overview of the model built into ABAQUS software

In Equations (5) and (6), p is the force applied to the end of the beam, L is the distance from the beam to the column, h_t is the distance to the center of the beam flange, H is the height of the column, Δ is the diameter of panel zones, d_{pz} , b_{pz} are the vertical and horizontal spacing of panel zones, respectively. Figure 5 shows the parameters in the connection source.

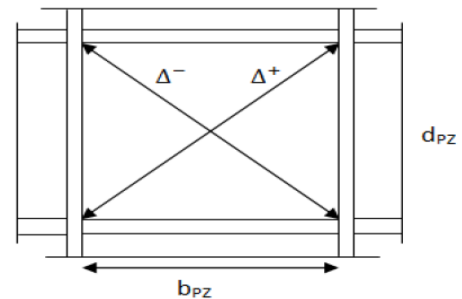
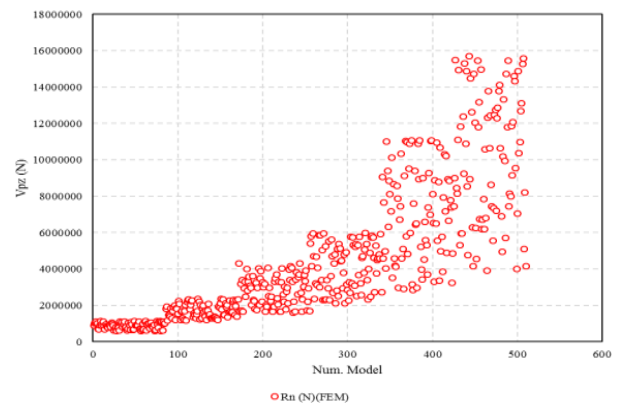
Figure 6 shows the calculated values of shear capacity in ABAQUS software and Equations (5) and (6) for 510 samples.

4. NN DESIGN AND GA TO PREDICT SHEAR CAPACITY OF THE CONNECTION SOURCE

4. 1. NN Design

In general, there are several types of NNs. The study will use a "Feedforward NN" or "Perception NNs". This ANN relays data directly from front to back. Feedforward neuron training often requires back-propagation, which is a network of corresponding sets of inputs and outputs. When the input data is transferred to the neuron, it is processed and an output is generated. Basically, a NN is a combination of the following components:

- An input layer that receives the data
- Several hidden layers

**Figure 5.** Details of the parameters in the connection source**Figure 6.** Shear capacity values in ABAQUS software for 510 samples

- An output layer
- Weights and bias between layers
- A deliberate activation function for each hidden layer. In this paper, the function of "tangent sigmoid" (tansig) will be used. This function maps each value to a value from 0 to 1 and helps to normalize the sum of the input weights [21].

In this step, the NN is trained to make accurate predictions. Each input will have a weight (positive or negative). This implies that an input with a large number of positive weights or a large number of negative weights will further influence the output result. It should also be remembered that initializing the weights by assigning a random number to any weight will happen. At each step, 9 geometric variables were assigned to 9 input layer neurons for training. Output data from ABAQUS software, we will have one number for every 9 inputs, introduced for training on NN. It should be noted that 510 samples are available as databases in this section. In other words, we will have 510 data outputs from ABAQUS as target and 510 * 9 data as input. 70% of this data was used for training, 10% for validating or averaging, and 20% for NN testing. For this problem, after trial and error, 6 hidden layers were considered. The next step was to determine the number of neurons in each layer. Each sample has 9 inputs and 1 output. As a result, we will have 9 neurons in the input layer and 1 neuron in the output layer. The number of neurons for secretary layers 1-6 was considered equal to 20, 30, 45, 35, 25 and 10. After several trials and errors, these neurons were selected to specify the number of layers. In the next step, it was necessary to specify the activation functions of each layer. By selecting the appropriate activation function for a layer, this activation function applied to all neurons in the same layer. Table 3 shows the used functions.

For the data of this paper, the tansig function (Sigmoid tangent) was used for individual layers and the purelin activation function (pair) for even layers, which showed relatively good convergence in outputs. Figure 7 shows the NN training process for training, test and intermediate data.

The four categories of data examined in this form are training data, test data, midterm data, and finally total data. Figure 8 shows the normal distribution of the error as a histogram during the training process.

4. 2. GA Design and Optimization As a computational optimization algorithm, by considering a

TABLE 3. Activation functions for each NN layer

No.	First layer	Second layer	Third layer	Fourth layer	Fifth layer	Sixth layer
Activation function	tansig	purelin	tansig	purelin	tansig	purelin

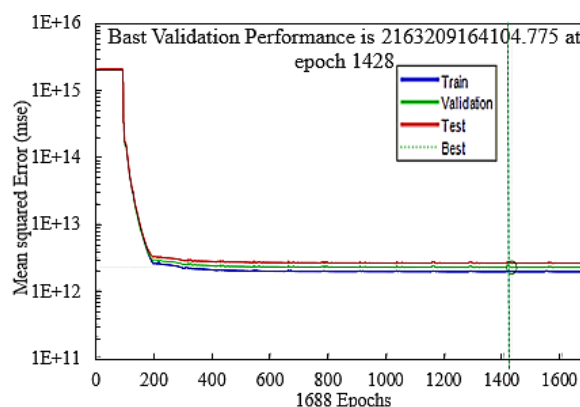


Figure 7. NN training diagram for training, test and intermediate data

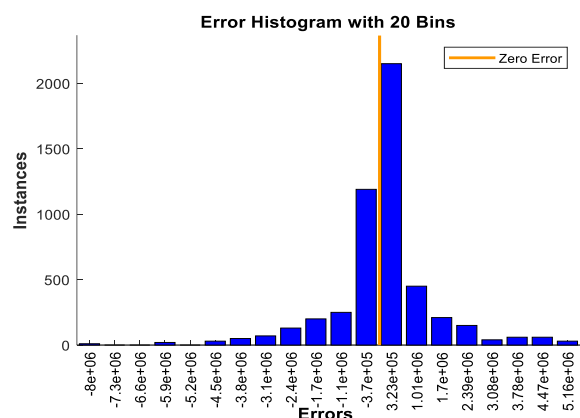


Figure 8. Histogram of error rate during training process for NN in the first case

set of answer space points in each computational iteration, the GA searches the different regions of the answer space efficiently. In the search mechanism, although the target function value of the whole answer space is not calculated, the calculated value of the target function for each point is involved in the statistical averaging of the objective function for each point, in the statistical averaging of the target function in all subfields to which the point depends is. These subfields are statistically averaged in terms of the objective function. This process leads the space search to areas where the statistical mean of the objective function is high and the possibility of an absolute optimal point is greater. Because, unlike single-path methods, this method searches for an all-encompassing answer space, there is less chance of convergence to a local optimal point. This article uses the AISC Equation to derive shear capacity for system identification. In addition to the AISC equation, the combination of polynomial functions was also used to better identify different states. Equation (7) is the equation that the GA seeks to optimize by applying changes in the values of the a_i coefficients. In this

equation, the x_i represents the inputs. It should be noted that by deriving a common denominator of Equation (7) and simplification, we arrive at a linear equation. However, this practice is not defined for the GA. In other words, the response of the algorithm to the linear function obtained from the simplification of Equation (7) will be different from the answer to Equation (7) itself. Table 4 shows coefficients 1-9 of the three optimized algorithms. In general, the outputs of the GA are expressed in three different states, namely the output of the project for one, two and three GAs that will work concurrently.

$$y \approx \sum_{i=1}^9 \alpha_i (x_i + \frac{x_i^3}{x_i^2}) \quad (7)$$

5. VALIDATION AND COMPARISON OF RESULTS

A series of graphs are plotted as colored contours, each of which determines the percentage error of the data part. In Figures 9-12, the percentage of NN output error and the GA are shown with the actual value. Taking a look at these color contours and the calculated error rate in each house from this checkerboard, we find that the GA worked well. Only one error point represents about 80% and most points below 10%.

To evaluate the performance of the networks, the mean squared error (MSE) method with an ideal value of zero was used. Mean Square Error (MSE) is one of the

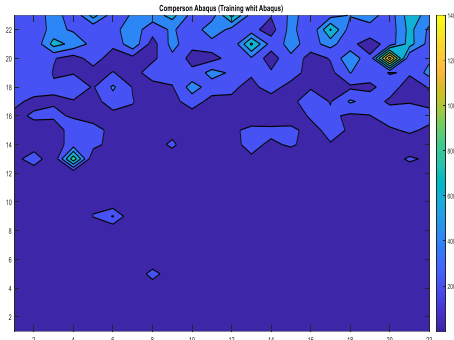


Figure 10. Comparison of the NN output with the actual output value of ABAQUS software as thermal graph

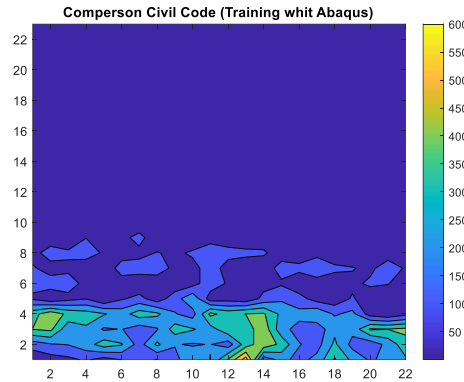


Figure 11. Comparison of the output of the NN with the output value of the AISC as a thermal graph

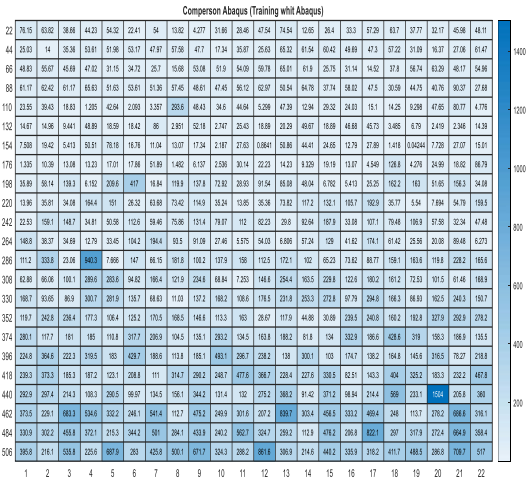


Figure 9. NN Output Error Percentage with Real Value (ABAQUS Software)

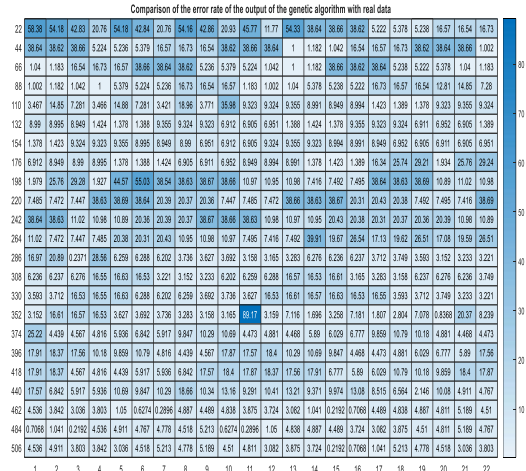


Figure 12. GA Output Error Percentage with Real Value (ABAQUS Software)

TABLE 4. Coefficients 1-9 of the three optimized algorithms

	α_9	α_8	α_7	α_6	α_5	α_4	α_3	α_2	α_1
Algorithm 1	49.21	49.22	49.08	2.52×10^{-5}	0.0019	678.38	532.64	2.68×10^{-5}	3.85×10^{-5}
Algorithm 2	90.35	90.71	88.26	0.0013	0.0012	42.61	238.70	0.0014	0.0005
Algorithm 3	98.55	97.67	90.012	0.0042	0.0316	38.54	40.65	0.0074	0.0033

statistical tools for finding prediction accuracy in modeling [21].

$$MSE = \sum_1^n \frac{(obs-calc)^2}{N} \tag{8}$$

N is Total number of training and test data pairs, obs is Training data, and Calc is Test data corresponding to training data. In this comparison, the data are divided into two categories. The first category relates to training data. This input data together with their response is provided to the smart method. Then, try to test the prediction performance using the second set of data, namely X data. Therefore, it is generally expected that the error of the training data is less than the test data. This is well seen in both Figures 13 and 14. In Figure 15, the error rate between the output of the NN and the output of the GA for ABAQUS data is calculated and shown.

The first point to note is the low error of prediction of the results by the GA compared to the NN in all different modes. This suggests that the choice of GA would be more appropriate in this particular case.

6. SENSITIVITY ANALYSIS

For sensitivity analysis, all input data were normalized to the range of 0 to 1. These parameters include column flange thickness, column web thickness, beam flange thickness, column width, height of beam and thickness of

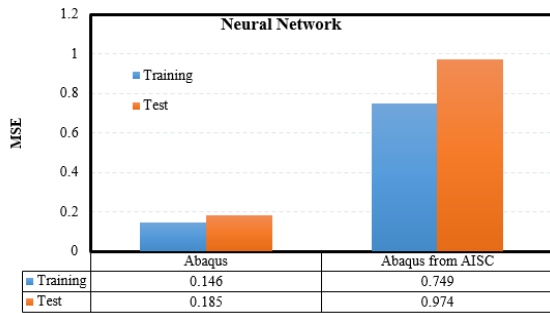


Figure 13. Values of the MSE NN

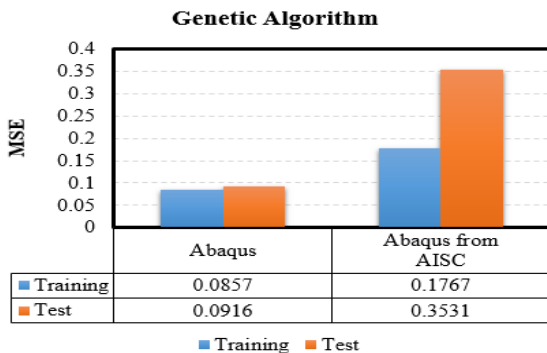


Figure 14. Values of the MSE GA

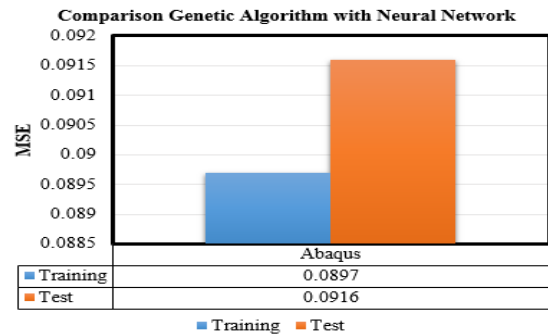


Figure 15. The error rate between the output of the NN and the output of the GA

continuity plates. The NN and GA are designed based on these parameters. If the output function is $f = R_n$, for the variations in the variable input, the input x_i is considered as follows:

$$\frac{\partial R_n}{\partial x_i} = \frac{f(x_i + \Delta x_i) - f(x_i - \Delta x_i)}{2\Delta x_i} \tag{9}$$

Considering $\Delta x_i = 0.05$, $\frac{\partial R_n}{\partial x_i}$ values were calculated as reported in Figure 16.

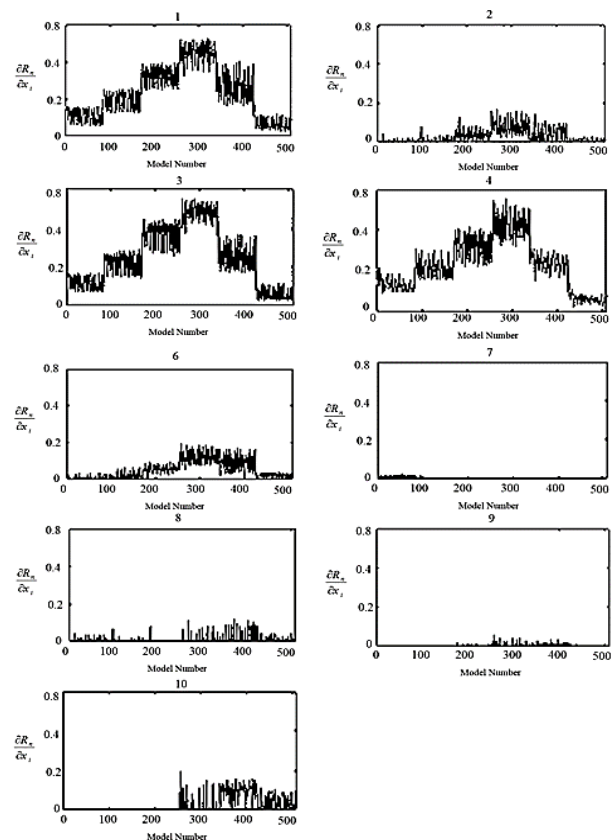


Figure 16. Sensitivity analysis for 9 parameters influencing the shear capacity of panel zone

In this figure, the x-axis represents 510 data and the y-axis represents $\frac{\partial R_n}{\partial x_i}$. The number shown at the top of each figure represents the input variable input. According to Figure 16, compared to other parameters, the three counters, namely 1, 3 and 4, are more effective in calculating the shear capacity. These parameters are column width, column thickness, flange and column web, respectively. This proves that the AISC relations are not efficient for calculating the shear capacity of panel zones at high thicknesses.

7. DISCUSSION AND CONCLUSION

In this comparison, the data are divided into two categories. The first category relates to training data. This input data is provided along with their response to the smart method. Then, we try to test the prediction performance using the second set of data, the X data. When ABAQUS data is selected as training and test data, smart methods perform best. However, in another case, if the test data are selected from the AISC data, the error rate will increase sharply. The present study presents a model using multilayer perceptron ANN and regression analysis method. This model is capable of measuring the shear capacity of a steel-shaped box-shaped column panel zone using 9 effective parameters (i.e., column length, column width, column flange thickness, column web thickness, beam width, beam height (X to X beam flange), beam flange thickness, beam web thickness, stiffener thickness). The results of the designed NN and GA refer to the following.

1) What is evident is the error of the AISC relations to determine the shear capacity of the box-shaped column panel zone. The AISC relations calculates shear capacity based on four parameters. However, the artificial intelligence networks in this study are trained on 9 parameters and predict the shear capacity of the coupling source, which reduces the error rate.

2) Sensitivity analysis based on a large parametric study of low to high thicknesses. In the AISC, the unstructured relations have shown that at high thicknesses, both the column thickness and the thickness of the bond plates affect the shear capacity. Therefore, by using the optimized equation of GA, a wide range of shear capacity of box-shaped columns with different column thicknesses can be obtained.

3) Artificial Intelligence Networks This study is based on 9 training parameters and predicts the shear capacity of the coupling source. Each of these AIs has errors with respect to ABAQUS output, which calculates the actual amount of shear capacity. Based on their performance evaluation, it can be concluded that the GA reduces the error to below 10% by using optimization.

8. REFERENCES

1. Arabzadeh, A., and Hizaji, R. "A Simple Approach to Predict the Shear Capacity and Failure Mode of Fix-ended Reinforced Concrete Deep Beams based on Experimental Study." *International Journal of Engineering, Transactions A: Basics*, Vol. 32, No. 4, (2019), 474–483. <https://doi.org/10.5829/ije.2019.32.04a.03>
2. AISC 360-05, Specification for structural steel buildings. Chicago(IL): American Institute of Steel Construction; (2010).
3. Mansouri, I., and Saffari, H. "A fast hybrid algorithm for nonlinear analysis of structures." *ASIAN Journal of Civil Engineering (BHRC)*, Vol. 15, No. 2, (2014), 213–229. <https://www.sid.ir/en/journal/ViewPaper.aspx?ID=353421>
4. Chithra, S., Kumar, S. R. R. S., Chinnaraju, K., and Alfin Ashmita, F. "A comparative study on the compressive strength prediction models for High Performance Concrete containing nano silica and copper slag using regression analysis and Artificial Neural Networks." *Construction and Building Materials*, Vol. 114, (2016), 528–535. <https://doi.org/10.1016/j.conbuildmat.2016.03.214>
5. Hartmann, S. "Project Scheduling with Multiple Modes: A Genetic Algorithm." *Annals of Operations Research*, Vol. 102, No. 1–4, (2001), 111–135. <https://doi.org/10.1023/A:1010902015091>
6. Elhewy, A. H., Mesbahi, E., and Pu, Y. "Reliability analysis of structures using neural network method." *Probabilistic Engineering Mechanics*, Vol. 21, No. 1, (2006), 44–53. <https://doi.org/10.1016/j.probengech.2005.07.002>
7. VANLUCHE, R. D., and SUN, R. "Neural Networks in Structural Engineering." *Computer-Aided Civil and Infrastructure Engineering*, Vol. 5, No. 3, (1990), 207–215. <https://doi.org/10.1111/j.1467-8667.1990.tb00377.x>
8. Jenkins, W. M. "Plane Frame Optimum Design Environment Based on Genetic Algorithm." *Journal of Structural Engineering*, Vol. 118, No. 11, (1992), 3103–3112. [https://doi.org/10.1061/\(ASCE\)0733-9445\(1992\)118:11\(3103\)](https://doi.org/10.1061/(ASCE)0733-9445(1992)118:11(3103))
9. Adeli, H. "Neural networks in civil engineering: 1989-2000." *Computer-Aided Civil and Infrastructure Engineering*, Vol. 16, No. 2, (2001), 126–142. <https://doi.org/10.1111/0885-9507.00219>
10. Sahoo, B., and Maity, D. "Damage assessment of structures using hybrid neuro-genetic algorithm." *Applied Soft Computing Journal*, Vol. 7, No. 1, (2007), 89–104. <https://doi.org/10.1016/j.asoc.2005.04.001>
11. Khalkhali, A., Nariman-Zadeh, N., Khakshournia, S., and Amiri, S. "Optimal Design of Sandwich Panels using Multi-objective Genetic Algorithm and Finite Element Method." *International Journal of Engineering, Transactions C: Aspects*, Vol. 27, No. 3, (2014), 395–402. <https://doi.org/10.5829/idosi.ije.2014.27.03c.06>
12. Mallela, U. K., and Upadhyay, A. "Buckling load prediction of laminated composite stiffened panels subjected to in-plane shear using artificial neural networks." *Thin-Walled Structures*, Vol. 102, (2016), 158–164. <https://doi.org/10.1016/j.tws.2016.01.025>
13. Abambres, M., and Lantsoght, E. O. L. "Neural network-based formula for shear capacity prediction of one-way slabs under concentrated loads." *Engineering Structures*, Vol. 211, (2020), 110501. <https://doi.org/10.1016/j.engstruct.2020.110501>
14. Hoang, N. D. "Estimating punching shear capacity of steel fibre reinforced concrete slabs using sequential piecewise multiple linear regression and artificial neural network." *Measurement: Journal of the International Measurement Confederation*, Vol.

- 137, (2019), 58–70. <https://doi.org/10.1016/j.measurement.2019.01.035>
15. Jang, B. W., and Kim, C. G. "Impact localization of composite stiffened panel with triangulation method using normalized magnitudes of fiber optic sensor signals." *Composite Structures*, Vol. 211, (2019), 522–529. <https://doi.org/10.1016/j.compstruct.2019.01.028>
16. Hedayat, A. A., Ahmadi Afzadi, E., Kalantaripour, H., Morshedi, E., and Iranpour, A. "A new predictive model for the minimum strength requirement of steel moment frames using artificial neural network." *Soil Dynamics and Earthquake Engineering*, Vol. 116, (2019), 69–81. <https://doi.org/10.1016/j.soildyn.2018.09.046>
17. Krawinkler, H., Popov, E., and Bertero, V. "Shear behavior of steel frame joints." *Journal of the Structural Division*, Vol. 101, No. 11, (1975), 2317–2336. Retrieved from <https://cedb.asce.org/CEDBsearch/record.jsp?dockkey=0006323>
18. Stojadinović, B., Goel, S. C., Lee, K. H., Margarian, A. G., and Choi, J. H. "Parametric tests on unreinforced steel moment connections." *Journal of Structural Engineering*, Vol. 126, No. 1, (2000), 40–49. [https://doi.org/10.1061/\(ASCE\)0733-9445\(2000\)126:1\(40\)](https://doi.org/10.1061/(ASCE)0733-9445(2000)126:1(40))
19. Mansouri, I., and Saffari, H. "A new steel panel zone model including axial force for thin to thick column flanges." *Steel and Composite Structures*, Vol. 16, No. 4, (2014), 417–436. <https://doi.org/10.12989/scs.2014.16.4.417>
20. Bayo, E., Loureiro, A., and Lopez, M. "Shear behaviour of trapezoidal column panels. I: Experiments and finite element modelling." *Journal of Constructional Steel Research*, Vol. 108, (2015), 60–69. <https://doi.org/10.1016/j.jcsr.2014.10.026>
21. Ho, S. L., Xie, M., and Goh, T. N. "A comparative study of neural network and Box-Jenkins ARIMA modeling in time series prediction." *Computers and Industrial Engineering*, Vol. 42, No. 3-4, 371–375. [https://doi.org/10.1016/S0360-8352\(02\)00036-0](https://doi.org/10.1016/S0360-8352(02)00036-0)

Persian Abstract

چکیده

بررسی رفتار چشمه اتصال ستون باکسی شکل یکی از مهمترین دغدغه‌های دانشمندان علم سازه بوده است. در آیین‌نامه فولاد آمریکا ظرفیت برشی مقاطع I شکل با ضخامت کم ستون محاسبه می‌شود. در این مقاله ظرفیت برشی چشمه اتصال در ستون‌های فلزی با مقاطع باکسی شکل با شبکه عصبی و الگوریتم ژنتیک تعیین می‌گردد و با خروجی‌های نرم‌افزار اجزا محدود آباکوس و روابط آیین‌نامه فولاد آمریکا مقایسه شده است. بنابراین با اطلاعات پارامتریک بدست آمده از ۵۱۰ مدل اتصال در نرم‌افزار آباکوس، شبکه عصبی آموزش داده شدند. نتایج نشان می‌دهد ظرفیت برشی که شبکه عصبی و الگوریتم ژنتیک پیش‌بینی می‌کند، طیف وسیعی از کلیه پارامترهای تاثیرگذار در محاسبه میزان ظرفیت برشی چشمه اتصال نسبت به روابط آیین‌نامه آمریکا استفاده می‌کند. بنابراین هوش‌های مصنوعی به کار رفته می‌تواند گزینه مناسبی باشد. در نهایت الگوریتم ژنتیک به همراه بهینه کردن یک رابطه ریاضی توانسته است میزان خطا را در تعیین ظرفیت برشی چشمه اتصال ستون‌های باکسی شکل فلزی حتی در ضخامت‌های بالای ستون به حداقل برساند.
